Analyses of displacement of the heart and its substructures caused by cardiac movement and identification of compensatory margins based on breath-hold electrocardiograph-gated 4-dimensional magnetic resonance imaging for oesophageal radiotherapy

Guanghui Yang
Shandong University
Chengrui Fu
Shandong Tumor Hospital and Institute
Guanzhong Gong
Shandong Tumor Hospital and Institute
Jing Zhang
Shandong Tumor Hospital and Institute
Qian Wang
Shandong Tumor Hospital and Institute
Chengxin Liu (liu.chengxin.2008@163.com)
Shandong University https://orcid.org/0000-0002-2296-7322
Baosheng Li
Shandong Tumor Hospital and Institute

Research

Keywords: 4-dimensional magnetic resonance imaging, cardiac movement, compensatory margin, oesophageal radiotherapy, radiation-induced heart disease

Posted Date: August 14th, 2020

DOI: https://doi.org/10.21203/rs.3.rs-58655/v1

Abstract

Background: Cardiac movement can affect the accuracy of the evaluation of the location of heart and its substructures by planning computed tomography (CT). We aimed to measure the margin displacement and calculate compensatory margins through breath-hold electrocardiograph (ECG)-gated 4-dimensional magnetic resonance imaging (4D-MRI) for oesophageal radiotherapy.

Methods: The study enrolled 10 patients with oesophageal radiotherapy plans and pretreatment 4D-MRI data. The displacement of the heart and its substructures was measured between the end of the systolic and diastolic phases in one cardiac cycle. The compensatory margins were calculated by extending the planning CT to cover the internal target volume (ITV) of all structures. Differences between groups were tested with the Kruskal-Wallis H test.

Results: The extent of movement of the heart and its substructures during one cardiac cycle were approximately 4.0-26.1 mm in the anterior-posterior (AP),left-right (LR), and cranial-caudal (CC) axes, and the compensatory margins should be applied to the planning CT by extending the margins by 1.7, 3.6, 1.8, 3.0, 2.1, and 2.9 mm for the pericardium, 1.2, 2.5, 1.0, 2.8, 1.8, and 3.3 mm for the heart, 3.8, 3.4, 3.1, 2.8, 0.9, and 2.0 mm for the interatrial septum, 3.3, 4.9, 2.0, 4.1, 1.1, and 2.9 mm for the interventricular septum, 2.2, 3.0, 1.1, 5.3, 1.8, and 2.4 mm for the left ventricular muscle (LVM), 5.9, 3.4, 2.1, 6.1, 5.4, and 3.6 mm for the antero-lateral papillary muscle (ALPM), and 6.6, 2.9, 2.6, 6.6, 3.9, and 4.8 mm for the postero-medial papillary muscle (PMPM) in the anterior, posterior, left, right, cranial, and caudal directions.

Conclusions: The locations of the heart and its substructures determined by planning CT were not able to represent the true positions due to cardiac movement, and compensatory margins can be applied to decrease the influence of movement.

1. Background

Radiotherapy has been considered an important treatment for thoracic tumours, but one of the disadvantages is radiation damage to the surrounding organs, such as the heart[1]. The heart was once considered a relatively radioresistant organ that was unlikely to be damaged when exposed to an irradiation dose of < 30 Gy, but the risk increased with exposure to doses > 40 Gy[2]. However, recent research has suggested that damage occurs even at moderate doses, and the rate of cardiac diseases increased after the atomic bomb imparted an average irradiation dose of 0.5-2 Gy[3]. Nonetheless, the specific threshold dose below which the heart would receive no damage is not yet known[4]. Irradiation damage to the heart frequently occurs during thoracic radiotherapy for oesophageal cancer, lung cancer, Hodgkin's disease, breast cancer, etc.[2, 5]. As the survival time of oesophageal cancer patients has been prolonged after radiotherapy, radiation-induced heart disease (RIHD) has attracted more attention because of its influence on survival. RIHD encompassed a series of effects on the heart, from subclinical histopathological findings to clinical disease, including damage to the pericardium, myocardium, valves, conduction system and coronary arteries. The exposed dose and volume were indicated to be major RIHD-related factors[6]. Dose-volume parameters based on planning computed tomography (CT) scans are currently considered the main method to predict RIHD.

In addition to respiratory movement[7, 8], the heart is especially influenced by periodic cardiac movement[9–11]. In some studies, it has been proven that assessments of the location of the heart and its substructures are

affected by movement. Tong et al. have calculated the displacements of 1.2 ± 0.9, 0.6 ± 0.5, and 0.6 ± 0.5 mm for the heart, 0.5 ± 0.4, 0.4 ± 0.3, and 0.8 ± 0.6 mm for the pericardium, and 1.0 ± 0.8, 4.1 ± 2.8, and 1.9 ± 1.2 for the left ventricular muscle (LVM) in the left-right, ventral-dorsal, and caudal-cranial directions by 4D-CT[9]. Tan et al. measured the average displacements of cardiac substructures and coronary arteries to be 3–8 mm[12]. Another study on displacements of the main coronary artery (CA) bifurcations measured that the movement of the margin in the AP, LR, and CC directions ranged from 4.6 to 21.8mm[10]. According to these studies, planning CT that displayed images of the heart instantly failed to represent the real morphology, volume and location of the heart and its substructures, and volume-dose parameters based on planning CT were inaccurate due to these displacements. Therefore, it is necessary to measure the displacement of the heart and its substructures accurately before radiotherapy for oesophageal radiotherapy.

At present, studies on the movement of the heart and its substructures are mostly based on cone-beam CT (CBCT), 4D-CT and other CT techniques; It is more challenging to delineate sophisticated substructures with these methods than with magnetic resonance imaging (MRI)[6]. Nevertheless, the application of planning MRI is limited due to the longer imaging time and financial burden. Thus, our research applied 4D-MRI to evaluate the dynamic changes during one cardiac cycle and calculated compensatory margins for planning CT that could improve the resolution of the heart and its substructures. The imaging process was combined with the breath-hold technique to reduce interference from respiratory movement and image artefacts. This research aims to provide more accurate heart protection and improve survival benefits for oesophageal cancer patients planning to undergo radiotherapy.

2. Methods

2.1 Patients

This study enrolled 10 patients with oesophageal radiotherapy plans and pretreatment 4D-MRI data from December 10th, 2018 to March 4th, 2020, including 1 female and 9 males aged from 59 to 77 years. All patients underwent breath-hold electrocardiograph (ECG)-gated 4D-MRI scanning before radiation treatment and did not have underlying heart disease. The study was approved by the Research Ethics Board of Shandong Cancer Hospital, and informed consent was provided by all patients.

2.2 ECG-gated 4D-MRI

Breath-hold ECG-gated 4D-MRI images were obtained with a GE Discovery MR750W device (General Electric Company, USA). The scan ranged from the level of the aortic arch to the bottom of the pericardium. The slice thickness was 5 mm, and the spacing was 0 mm. Radio-frequency excitation and signal acquisition were performed during MRI of the whole cardiac cycle. At the same time, ECG information was integrated into the MRI system. MR signals were used to reconstruct images in different phases, so the contraction and relaxation of the atria and ventricles could be observed in a “cine” mode. In this study, every 5% of the cardiac cycle was reconstructed into one phase, and 20 phases (0%, 5%, 10%...95%) in all were considered.

2.3 Planning CT

Patients were scanned by a Philips CT simulator in the supine position and immobilized with their hands above their heads holding the handles. Magnification markers were applied on the chest and both sides of the body. Plain and enhanced CT images were then transported to a Varian Eclipse 8.6.15 system (Varian Medical

Systems, USA) for radiation planning and design. Contrast-enhanced CT (CECT) images were used to contour the target volume, while plain CT images were used for planning and dose calculation. The planning CT images were then transported to a Varian Trilogy linear accelerator to facilitate radiation treatment after verification by clinicians.

2.4 Delineation Principles

The heart and its substructures mentioned above included the pericardium, heart, interatrial septum, interventricular septum, LVM, antero-lateral papillary muscle (ALPM) and postero-medial papillary muscle (PMPM). The superior boundary of the pericardium started from the presence of the left superior pulmonary vein, and the inferior boundary ended where the pericardium fused with the diaphragm; the heart started from the presence of the left atrium and ended when the signals of the muscle tissue vanished, excluding the superior and inferior vena cava. The boundary between the LVM and interventricular septum was defined as the left margin of the right coronary anterior descending branch. The ALPM and PMPM were contoured separately. All images were contoured by the same clinician and verified by another clinician.

2.5 Data acquisition

Both planning CT and 4D-MRI images were transported to a commercial MIM Maestro 6.7.6 workstation (MIM Software Inc., Cleveland, OH, USA) for margin delineation. The displacement of the heart and its substructures was measured in the AP, LR, and CC axes between the end of the systolic and diastolic phases, which were usually considered the 10%-35% and 75%-85% phases. The compensatory margin was calculated by extending the margins of the heart and its substructures on the planning CT to overlap with the internal target volume (ITV) generated from 4D-MRI. ITV was defined as the target volume considering target movement (e.g., respiratory movement or cardiac movement).

2.6 Statistical Analysis

All data are presented as the mean ± standard deviation (mm). The differences between different groups were tested with the Kruskal-Wallis H test. Differences were considered significant at $p < 0.05$. Statistical analysis was conducted with SPSS 23.0 software (SPSS Inc., Chicago, IL).

3. Results

3.1 Displacement of the heart and its substructures

The displacements of the heart and its substructures in the AP, LR and CC directions were as follows (Table 1): interatrial septum: (18.4 ± 6.9), (16.4 ± 6.5), and (4.0 ± 3.2) mm; interventricular septum: (20.4 ± 7.6), (16.1 ± 5.2), and (4.5 ± 5.0) mm; LVM: (17.6 ± 5.9), (26.1 ± 5.8), and (4.0 ± 5.2) mm; ALPM: (17.3 ± 4.2), (14.3 ± 6.9), and (5.0 ± 6.2) mm; and PMPM: (19.7 ± 7.5), (9.8 ± 5.7), and (8.0 ± 7.5) mm, respectively. The displacements in the AP and LR directions were (9.9 ± 3.7) and (15.9 ± 6.7) mm for the pericardium and (19.5 ± 4.4) and (20.9 ± 5.5) mm for the heart, respectively; movements of the pericardium and heart in the CC direction failed to be observed due to the limited imaging range of 4D-MRI. According to our data, the displacement of the heart and other substructures basically ranged from 4 mm to 20 mm, implying that the margin displacement influenced by periodic cardiac movement was nonnegligible. Interestingly, although the size of the left ventricular papillary muscles was smaller than that of the other structures, the motion amplitude showed no significant differences

among structures (P = 0.423, 0.423, 0.406 respectively in AP, LR, and CC axes). The movement of the pericardium was significantly milder in the AP direction than that of other structures. The most obvious movement was for the LVM in the LR direction, which might be related to LVM systolic and diastolic deformation during the ejection of blood.

3.2 The Compensatory Margin For Planning Ct

From the images, the edge of the ITV of each structure was basically located outside that on the planning CT. The mean ITV was larger than the planning CT volume (Table 2): pericardium: 743.39 vs. 726.62 (ml), heart: 547.94 vs. 546.53 (ml), interatrial septum: 11.93 vs. 3.71 (ml), interventricular septum: 59.79 vs. 28.45 (ml), LVM: 99.96 vs. 51.25 (ml), ALPM: 6.8 vs. 1.01 (ml), and PMPM: 5.09 vs. 0.62. The compensatory margin would extend the margin of the planning CT in six directions (anterior, posterior, left, right, cranial, and caudal) by the following distances: pericardium: (1.7 ± 0.9), (3.6 ± 1.6), (1.8 ± 1.6), (3.0 ± 1.7), (2.1 ± 3.5), and(2.9 ± 2.7) mm; heart: (1.2 ± 1.0), (2.5 ± 1.7), (1.0 ± 0.7), (2.8 ± 1.2), (1.8 ± 3.4), and (3.3 ± 2.9) mm; interatrial septum: (3.8 ± 2.6), (3.4 ± 2.9), (3.1 ± 1.7), (2.8 ± 1.6), (0.9 ± 1.8), and (2.0 ± 3.9) mm; interventricular septum: (3.3 ± 1.7), (4.9 ± 2.4), (2.0 ± 1.9), (4.1 ± 1.9), (1.1 ± 1.8), and (2.9 ± 3.7) mm; LVM: (2.2 ± 1.6), (3.0 ± 1.6), (1.1 ± 0.8), (5.3 ± 2.0), (1.8 ± 2.4), and(2.4 ± 3.5) mm; ALPM: (5.9 ± 3.5), (3.4 ± 2.5), (2.1 ± 1.5), (6.1 ± 2.4), (5.4 ± 4.2), and (3.6 ± 3.2) mm; and PMPM: (6.6 ± 2.7), (2.9 ± 2.2), (2.6 ± 2.5), (6.6 ± 2.7), (3.9 ± 4.1), and(4.8 ± 5.1) mm, respectively (Table 3). The extent of the compensatory margin was obviously smaller than the displacement, ranging from approximately 1 to 6 mm. The compensatory margins for the ALPM (mean value = 4.42 mm) and PMPM (mean value = 4.57 mm) were larger than those for the pericardium (mean value = 2.52 mm),heart(mean value = 2.10 mm) and LVM (mean value = 2.63 mm), with $P < 0.05$; this reflects the heterogeneity in the motion of the heart and its structures and reminds us that for patients with pretreatment left ventricular valve disfunction, the ALPM and PMPM should be separately contoured as organs at risk (OARs). Except for that for the ALPM, the compensatory extent for the other structures were larger in the caudal direction than in the cranial direction. Except for that for the interatrial septum, the extent of the compensatory margin was almost 2- to 5-fold higher in the right direction than in the left direction. According to the data, the planning CT cannot represent the true location and volume of the heart, and a compensatory margin should be applied on planning CT to assess volume-dose parameters.

Table 1
Displacement of the heart and substructures (mm, mean ± standard deviation, range)

Structures	Pericardium	Heart	Interatrial septum	Interventricular septum	LVM	ALPM	PMPM
AP	9.9 ± 3.7(4.8–15.5)	19.5 ± 4.4(13.7–27.9)	18.4 ± 6.9(10.4–29.0)	20.4 ± 7.6(12.2–32.3)	17.6 ± 5.9(11.3–32.2)	17.3 ± 4.2(12.4–25.3)	19.7 ± 7.5(12.0-35.8)
LR	15.9 ± 6.7(5.7–29.0)	20.9 ± 5.5(12.0–28.0)	16.4 ± 6.5(5.9–27.9)	16.1 ± 5.2(10.7–27.4)	26.1 ± 5.8(19.1–35.1)	14.3 ± 6.9(6.3–25.5)	9.8 ± 5.7(2.3–22.2)
CC	-	-	4.0 ± 3.2(0.0–10.0)	4.5 ± 5.0(0.0–15.0)	4.0 ± 5.2(0.0–15.0)	5.0 ± 6.2(0.0–20.0)	8.0 ± 7.5(0.0–25.0)

Abbreviations: AP = anterior-posterior, LR = left-right, CC = cranial-caudal, LVM = left ventricular muscle, ALPM = antero-lateral papillary muscle, PMPM = postero-medial papillary muscle.

Movement of the pericardium and heart in the CC direction was not observable due to the imaging range of 4D-MRI.

Table 2
The mean ITV and planning CT volumes of the heart and its substructures (ml)

Structures	Pericardium	Heart	Interatrial septum	Interventricular septum	LVM	ALPM	PMPM
ITV	743.39	547.94	11.93	59.79	99.96	6.8	5.09
Planning CT	726.62	546.53	3.71	28.45	51.25	1.01	0.62

Abbreviations: LVM = left ventricular muscle, ALPM = antero-lateral papillary muscle, PMPM = postero-medial papillary muscle, ITV = internal target volume.

Table 3
Compensatory margin extensions in order to overlap with the ITV (mm, mean ± standard deviation, range)

Structures	Pericardium	Heart	Interatrial septum	Interventricular septum	LVM	ALPM	PMPM
Anterior	1.7 ± 0.9(0.0–3.0)	1.2 ± 1.0(1.0–3.0)	3.8 ± 2.6(0.0–7.0)	3.3 ± 1.7(0.0–6.0)	2.2 ± 1.6(0.0–4.0)	5.9 ± 3.5(2.0–12.0)	6.6 ± 2.7(2.0–9.0)
Posterior	3.6 ± 1.6(0.0–5.0)	2.5 ± 1.7(0.0–6.0)	3.4 ± 2.9(0.0–8.0)	4.9 ± 2.4(1.0–9.0)	3.0 ± 1.6(1.0–6.0)	3.4 ± 2.5(0.0–9.0)	2.9 ± 2.2(0.0–6.0)
Left	1.8 ± 1.6(0.0–4.0)	1.0 ± 0.7(0.0–2.0)	3.1 ± 1.7(1.0–5.0)	2.0 ± 1.9(1.0–7.0)	1.1 ± 0.8(0.0–2.0)	2.1 ± 1.5(0.0–5.0)	2.6 ± 2.5(0.0–7.0)
Right	3.0 ± 1.7(0.0–4.0)	2.8 ± 1.2(1.0–5.0)	2.8 ± 1.6(1.0–6.0)	4.1 ± 1.9(1.0–6.0)	5.3 ± 2.0(3.0–9.0)	6.1 ± 2.4(3.0–10.0)	6.6 ± 2.7(0.0–9.0)
Cranial	2.1 ± 3.5(0.0–5.0)	1.8 ± 3.4(0.0–4.0)	0.9 ± 1.8(0.0–5.0)	1.1 ± 1.8(0.0–4.0)	1.8 ± 2.4(0.0–6.0)	5.4 ± 4.2(0.0–12.0)	3.9 ± 4.1(0.0–12.0)
Caudal	2.9 ± 2.7(0.0–7.0)	3.3 ± 2.9(0.0–7.0)	2.0 ± 3.9(0.0–12.0)	2.9 ± 3.7(0.0–10.0)	2.4 ± 3.5(0.0–5.0)	3.6 ± 3.2(0.0–8.0)	4.8 ± 5.1(0.0–12.0)

Abbreviations: LVM = left ventricular muscle, ALPM = antero-lateral papillary muscle, PMPM = postero-medial papillary muscle. The data above are shown in millimetres (mm).

4. Discussion

Radiotherapy has led to survival benefits for thoracic cancers, such as breast cancer, Hodgkin's lymphoma (HL), oesophageal cancer and lung cancer. However, because of the longer survival period, the risk of RIHD has

increased. A study involving 1474 HL patients reported that the RR in post-radiation patients ranged from 3 to 5, and 66–80% of patients suffered from RIHD induced by mediastinal radiation[13]. Cardiac-induced mortality was the leading cause of non-cancer-induced death in both HL and breast cancer after radiotherapy[13]. Relatively fewer studies have focused on RIHD of oesophageal cancer than on HL and breast cancer because the survival period of oesophageal cancer is obviously shorter. However, the dose to the heart during oesophageal radiotherapy is elevated because of the anatomical location. The mean dose received by the heart in breast cancer is commonly 10–15 Gy, while in distal oesophageal radiotherapy, this dose might reach or exceed 50 Gy[14]. Beukema et al. collected articles published from 1970–2013 related to cardiotoxicity after oesophageal cancer radiotherapy and found that the rate of RHID was approximately 10.8% (5–44%) [15]. Ogino et al. conducted a retrospective study with a median follow-up period of 79 months (range from 48–127 months), and 343 oesophageal cancer patients who received concurrent radiotherapy or radiotherapy alone with long-term survival (more than 4 years) were included. The end point of the study was symptomatic heart disease, with a five-year incidence of 13.8%[16].

The clinical spectra of heart diseases caused by radiotherapy include pericardial disease, myocarditis, valvular disease, coronary artery disease (CAD) and conduction abnormalities. Pericardium effusion and pericarditis are the most common RIHDs. Pericardium effusion is usually asymptomatic. Acute pericarditis mostly occurs during or after radiotherapy, while delayed chronic pericarditis usually occurs 1 year after treatment[17]. The main mechanism of myocardial damage was fibrosis, which might lead to congestive insufficiency. Most chronic heart failure occurred decades after treatment[1]. CAD is rare in RIHD but is fatal, with a latent period of approximately 10 years. Radiation-induced valvular disease mainly influences the left ventricle[5]. Valvular disease involves valvular contraction and regurgitation. Regurgitation symptoms are more common and usually occur 10 years post-radiation. In a study by Lund et al., the incidence of left ventricular valve regurgitation in patients with HL after radiotherapy was 6–40%, compared with 2% in patients without radiotherapy[18]. The pathological basis of conduction system disorder was also fibrosis induced by irradiation. The manifestation of conduction system disorder is ECG abnormalities, and approximately 70% of patients returned to normal ECG readings without intervention. Other than acute pericarditis, most RIHDs have a relatively long incubation period, and the incidence increases with time.

The two major risk factors of RIHD include irradiation dose and volume[6]. According to a long-term follow-up of 4414 post-radiation breast cancer patients by Honning et al., the rate of RIHD was related to the mean dose to the heart during radiotherapy[19]. Another study of RIHD in breast cancer put forward a specific dosimetric relationship between delivered dose and rate of cardiac mortality, which increased by 3% for every additional 1 Gy of radiation dose[4]. Carmel et al. proved that the rate of pericarditis induced by entire heart irradiation was able to be decreased by blocking the left ventricle and inferior pericardium region[20]. All of this research implies the importance of evaluating the displacement of the heart and its substructures, which would influence the irradiation dose and volume. Apart from these, factors such as fraction dose, radiotherapy techniques, chemotherapeutic agents (mainly anthracyclines and trastuzumab), and patient risk factors such as age have also been proven to be related to RIHD. With the development of radiotherapy technology, the cardiotoxicity of radiotherapy has been significantly reduced. According to Lin SH et al., compared with 3-dimensional conformal radiotherapy (3D-CRT), intensity modulated radiation therapy (IMRT) remarkably reduced cardiac mortality (72.6% vs 52.9%, $P < 0.001$), but cancer-specific mortality showed no significant difference between methods ($P = 0.86$)[21]. However, the risk of cardiotoxicity has not been eliminated by techniques at present[22].

Anthracyclines are commonly used as chemotherapy schemes in the treatment of breast cancer and HL patients. The most frequent regimen of concurrent radiochemotherapy for oesophageal cancer is 5-FU and cisplatin, which have also been proven to be slightly cardiotoxic[23, 24].

Thus, it is necessary to accurately evaluate the displacement of the heart and its substructures caused by periodic cardiac activity and calculate the compensatory margin that could be applied in clinical practice when creating a radiotherapy plan. Many studies have proven that delineation of the pericardium, heart, LVM, and CA system based on planning CT fails to show the real margin of the substructures mentioned above during the cardiac cycle[9–12], and a compensatory margin for planning CT should be applied. One study based on CBCT recommended compensatory margins of 11 (left), 6 (right), 3 (cranial), 4 (caudal), 7 (anterior), and 5 (posterior) mm for the heart. Kataria et al. measured that radial and cranio-caudal margins of 7 mm and 4 mm, respectively, would cover the range of motions of the CA on CECT [11]. Li et al. found that the maximum compensatory margins in the LR, CC, and AP directions for the CA bifurcations were 6, 6, and 5 mm (left) and 6, 8, and 7 mm (right) on 4D-CT, respectively[10]. Therefore, the volume-dose parameters used to evaluate the dose to the heart might not truly reflect the dose received during oesophageal radiotherapy and could not provide accurate protection for the heart. Studies on heart motion at present mostly focus on the entire heart and CA system based on CT, but the ability to distinguish sophisticated structures has been challenged. Considering that MRI has the advantage of discriminating muscular structures, we aimed to conduct research on the displacement of the pericardium, heart, interatrial septum, interventricular septum, LVM, ALPM and PMPM with 4D-MRI. With the application of the breath-hold technique, the influence of respiratory movement was offset.

Based on our results, the displacement of the whole heart and its substructures caused by cardiac activity was non-negligible, ranging from 4 mm to 26.1 mm. The most significant motion was in the LR direction for the LVM (26.1 mm). The amplitude of pericardium motion was slightly milder than the motion of the LVM, interatrial septum and interventricular septum. Considering that position, volume and morphology changed during the cardiac cycle, we then reconstructed the ITV, which reflected the actual locations based on 20 phases of 4D-MRI. Radiotherapy plans are still mainly designed and evaluated with CT images, so we hoped to provide specific compensatory margins for planning CT to make the recommendations more realistic. Because of the periodic cardiac movement, the ITV that reflected the extent of motion could be larger than the volume contoured on the planning CT for every structure mentioned above theoretically. Consistent with the hypothesis, the ITV boundary of each structure was larger than that contoured on the planning CT, and the compensatory margins ranged from 0.9 mm to 6.6 mm. The volume differences of the pericardium (743.39 ml vs. 726.62 ml) and heart (547.94 ml vs. 546.53 ml) were moderate, while for other structures, the largest difference could as high as an eight-fold difference. The largest differences between the ITV and planning CT volume were for the ALPM and PMPM. This was consistent with the trend that the motion amplitude of the left ventricular papillary muscles was similar to that of other structures ($P = 0.423$, 0.423, 0.406 respectively in AP, LR, and CC axes), even though these muscles have a much smaller volume. The largest compensatory distance was for the left ventricular papillary muscle. There were no significant differences among the motion amplitudes of the involved substructures, but the compensatory distances were significantly different ($P = 0.044$). Through further analysis, disparities mainly existed between the heart and ALPM ($P = 0.008$), heart and PMPM ($P = 0.008$), LVM and ALPM ($P = 0.039$), LVM and PMPM ($P = 0.038$), pericardium and ALPM ($P = 0.041$) and pericardium and PMPM ($P = 0.039$). It could be prompted that the left ventricular papillary muscles were more active and that it was more difficult to assess the potential exposure to these muscles with the dose-volume parameters based on planning CT. Part of the reason

might be the low resolution of the papillary muscles on CT images, suggesting that the boundary of the papillary muscles contoured on the planning CT might be smaller than the real volume. In conclusion, according to our study, it is necessary to evaluate cardiac radiation exposure by applying compensatory margins on planning CT for a high-risk population who might have symptomatic cardiac damage during thoracic radiation.

Our research had the advantage of applying the breath-hold ECG-gated 4D-MRI technique, as well as focusing on substructures of the heart. However, the research was also limited by the sample size, which led to a relatively large deviation. As a result of a narrow imaging range, the inferior margin of the pericardium and the whole heart were not completely displayed on 4D-MR, which made it impossible to measure the motion amplitude of the pericardium and heart, and their compensatory margins might be smaller than those actually needed. The standard compensatory margins of the heart and its substructures require verification in more clinical trials. This research concentrated on displacement of the heart and its substructures and compensatory margins only, and future research of dose-volume parameters during oesophageal radiotherapy based on 4D-MRI should be conducted.

5. Conclusion

In summary, because of cardiac cycle motion, the margin displacement of the heart and its substructures were quite obvious, making it inappropriate to apply the delineations from planning CT to assess heart exposure in during oesophageal radiotherapy, especially for patients with underlying heart disease. According to the present research, compensatory margins should be applied to the planning CT by extending the margins in the anterior, posterior, left, right, cranial, and caudal directions, specifically by 1.7, 3.6, 1.8, 3.0, 2.1, and 2.9 mm for the pericardium, 1.2, 2.5, 1.0, 2.8, 1.8, and 3.3 mm for the heart, 3.8, 3.4, 3.1, 2.8, 0.9, and 2.0 mm for the interatrial septum, 3.3, 4.9, 2.0, 4.1, 1.1, and 2.9 mm for the interventricular septum, 2.2, 3.0, 1.1, 5.3, 1.8, and 2.4 mm for the LVM, 5.9, 3.4, 2.1, 6.1, 5.4, and 3.6 mm for the ALPM and 6.6, 2.9, 2.6, 6.6, 3.9, and 4.8 mm for the PMPM.

Abbreviations

CT = computed tomography, ECG = electrocardiograph, 4D-MRI = 4-dimensional magnetic resonance imaging, LVM = left ventricular muscle, ALPM = antero-lateral papillary muscle, PMPM = postero-medial papillary muscle, AP = anterior-posterior, LR = left-right, CC = cranial-caudal, ITV = internal target volume, RIHD = radiation-induced heart disease, CECT = contrast-enhanced computed tomography, OAR = organ at risk, RR = relative risk, HL = Hodgkin's lymphoma, CAD = coronary artery disease.

Declarations

Conflict of interest

All the authors declare that no conflicts of interest exist.

Availability of data and materials

The dataset used and analysed during the current study is available from the corresponding author on reasonable request.

Ethics approval and consent to participate

This study was approved by the Research Ethics Board of Shandong Cancer Hospital, and informed consent was provided by all patients.

Consent for publication

All authors gave their consent for publication.

Competing interests

The authors declare that they had no competing interests.

Funding

This work was supported by the Natural science foundation of shandong province (grant number ZR2016HP32).

Authors' contributions

GHY and CRF participated in the study design, collected the clinical data, performed the statistical analysis and delineations and drafted the manuscript. GZG verified the delineation and offered physical support. QW and JZ supported the statistical analysis. BSL and CXL conceived the study, participated in its design and revised the manuscript. All authors read and approved the final manuscript.

Acknowledgements

During the protocol designing, data collecting and analyzing, and the manuscript writing, tremendous supports had been being from clinical and technique colleagues. Their supports and helps should be appreciated.

References

1. Wang H, Wei J, Zheng Q, Meng L, Xin Y, Yin X, et al. Radiation-induced heart disease: a review of classification, mechanism and prevention. Int J Biol Sci. 2019;15(10):2128-38.
2. Selwyn AP. The cardiovascular system and radiation. Lancet. 1983;ii:152–4.
3. Shimizu Y, Kodama K, Nishi N, Kasagi F, Suyama A, Soda M, et al. Radiation exposure and circulatory disease risk: Hiroshima and Nagasaki atomic bomb survivor data, 1950-2003. BMJ. 2010;340:b5349.
4. Darby SC, Cutter DJ, Boerma M, Constine LS, Fajardo LF, Kodama K, et al. Radiation-related heart disease: current knowledge and future prospects. Int J Radiat Oncol Biol Phys. 2010;76(3):656-65.
5. Heidenreich PA, Kapoor JR. Radiation induced heart disease: systemic disorders in heart disease. Heart. 2009;95(3):252-8.
6. Gagliardi G, Constine LS, Moiseenko V, Correa C, Pierce LJ, Allen AM, et al. Radiation dose-volume effects in the heart. Int J Radiat Oncol Biol Phys. 2010;76(3 Suppl):S77-85.
7. Topolnjak R, Borst GR, Nijkamp J, Sonke JJ. Image-guided radiotherapy for left-sided breast cancer patients: geometrical uncertainty of the heart. Int J Radiat Oncol Biol Phys. 2012;82(4):e647-55.

8. Qi XS, Hu A, Wang K, Newman F, Crosby M, Hu B, et al. Respiration induced heart motion and indications of gated delivery for left-sided breast irradiation. Int J Radiat Oncol Biol Phys. 2012;82(5):1605-11.
9. Tong Y, Yin Y, Lu J, Liu T, Chen J, Cheng P, et al. Quantification of heart, pericardium, and left ventricular myocardium movements during the cardiac cycle for thoracic tumor radiotherapy. Onco Targets Ther. 2018;11:547-54.
10. Li Q, Tong Y, Yin Y, Cheng P, Gong G. Definition of the margin of major coronary artery bifurcations during radiotherapy with electrocardiograph-gated 4D-CT. Physica Medica. 2018;49:90-4.
11. Kataria T, Bisht SS, Gupta D, Abhishek A, Basu T, Narang K, et al. Quantification of coronary artery motion and internal risk volume from ECG gated radiotherapy planning scans. Radiother Oncol. 2016;121(1):59-63.
12. Tan W, Xu L, Wang X, Qiu D, Han G, Hu D. Estimation of the displacement of cardiac substructures and the motion of the coronary arteries using electrocardiographic gating. Onco Targets Ther. 2013;6:1325-32.
13. Aleman BM, van den Belt-Dusebout AW, De Bruin ML, van 't Veer MB, Baaijens MH, de Boer JP, et al. Late cardiotoxicity after treatment for Hodgkin lymphoma. Blood. 2007;109(5):1878-86.
14. Minsky BD, Pajak TF, Ginsberg RJ, Pisansky TM, Martenson JA, Komaki R, et al. INT 0123 (Radiation Therapy Oncology Group 94-05) Phase III Trial of Combined-Modality Therapy for Esophageal Cancer: High-Dose Versus Standard-Dose Radiation Therapy. J Clin Oncol. 2002;20(5):1167-74.
15. Beukema JC, van Luijk P, Widder J, Langendijk JA, Muijs CT. Is cardiac toxicity a relevant issue in the radiation treatment of esophageal cancer? Radiother Oncol. 2015;114(1):85-90.
16. Ogino I, Watanabe S, Iwahashi N, Kosuge M, Sakamaki K, Kunisaki C, et al. Symptomatic radiation-induced cardiac disease in long-term survivors of esophageal cancer. Strahlenther Onkol. 2016;192(6):359-67.
17. Madan R, Benson R, Sharma DN, Julka PK, Rath GK. Radiation induced heart disease: Pathogenesis, management and review literature. *J Egypt Natl Canc Inst*. 2015;27(4):187-93.
18. Lund MB, Ihlen H, Voss BMR, Abrahamsen AF, Nome O, Kongerud J, et al. Increased risk of heart valve regurgitation after mediastinal radiation for Hodgkin's disease: an echocardiographic study. Heart. 1996;75(6):591-5.
19. Hooning MJ, Botma A, Aleman BM, Baaijens MH, Bartelink H, Klijn JG, et al. Long-term risk of cardiovascular disease in 10-year survivors of breast cancer. J Natl Cancer Inst. 2007;99(5):365-75.
20. Carmel RJ, Kaplan HS. Mantle irradiation in Hodgkin's disease. An analysis of technique, tumor eradication, and complications. Cancer. 1976;37(6):2813-2825.
21. Lin SH, Wang L, Myles B, Thall PF, Hofstetter WL, Swisher SG, et al. Propensity Score-based Comparison of Long-term Outcomes With 3-Dimensional Conformal Radiotherapy vs Intensity-Modulated Radiotherapy for Esophageal Cancer. *Int J Radiat Oncol Biol Phys*. 2012;84(5):1078-85.
22. Boero IJ, Paravati AJ, Triplett DP, Hwang L, Matsuno RK, Gillespie EF, et al. Modern Radiation Therapy and Cardiac Outcomes in Breast Cancer. Int J Radiat Oncol Biol Phys. 2016;94(4):700-8.
23. Schlitt A, Jordan K, Vordermark D, Schwamborn J, Langer T, Thomssen C. Cardiotoxicity and oncological treatments. Dtsch Arztebl Int. 2014;111(10):161-8.
24. Patane S. Cardiotoxicity: cisplatin and long-term cancer survivors. Int J Cardiol. 2014;175(1):201-2.

Figures

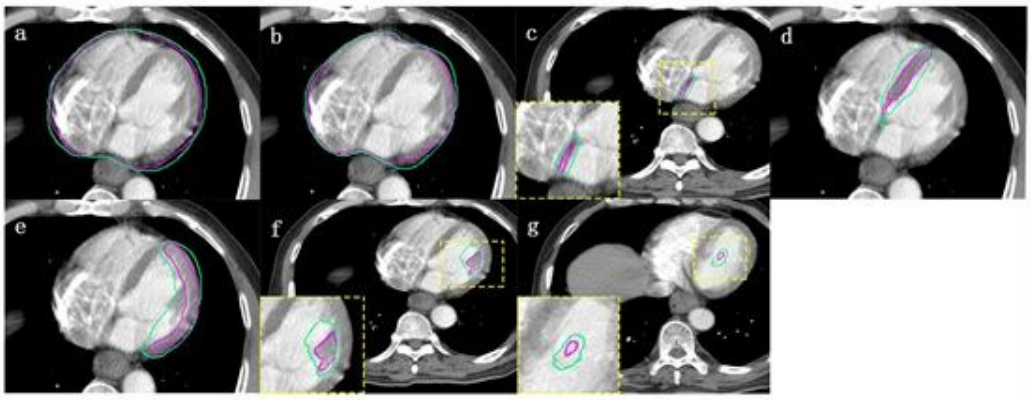

Fig. 1 The ITV boundaries are shown in green, and the delineation based on the planning CT is shown in purple. Images a-g show the motion of the margins of the pericardium, heart, interatrial septum, interventricular septum, LVM, ALPM, and PMPM. All images are from the same level in the same patient except for those of the PMPM due to its anatomical location. We chose the four-chamber level to display as many substructures as possible.

Figure 1

(caption included in figure)

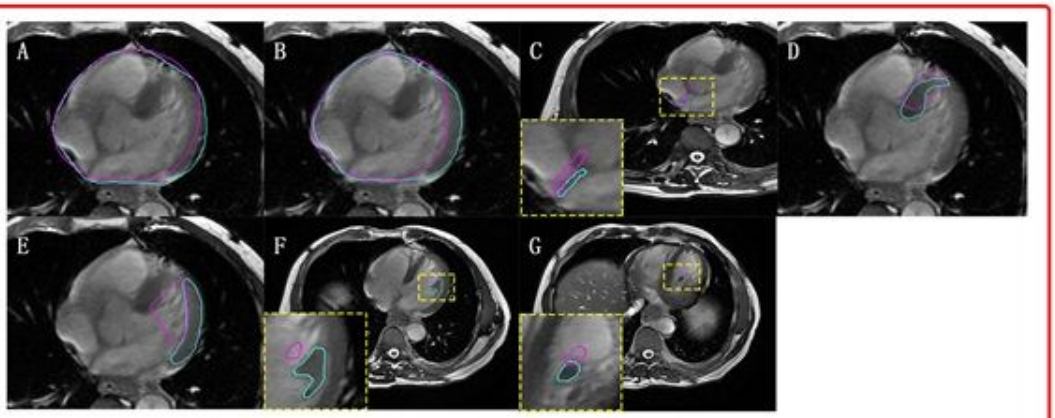

Fig. 2 The delineation in the 10% phase (purple line) and 70% phase (blue line) represent the end of the systolic and diastolic phases, respectively. Images A-G show the motion of the margins of the pericardium, heart, interatrial septum, interventricular septum, LVM, ALPM, and PMPMP of the same patient separately.

Figure 2

(caption included in figure)